Inverse full state hybrid projective synchronization for chaotic maps with different dimensions

Adel Ouannas[1,†] and Giuseppe Grassi[2,‡]

[1] Laboratory of Mathematics, Informatics and Systems (LAMIS), University of Larbi Tebessi, Tebessa 12002, Algeria
[2] Università del Salento, Dipartimento Ingegneria Innovazione, 73100 Lecce, Italy

(Received 22 November 2015; revised manuscript received 6 March 2016; published online 3 August 2016)

A new synchronization scheme for chaotic (hyperchaotic) maps with different dimensions is presented. Specifically, given a drive system map with dimension n and a response system with dimension m, the proposed approach enables each drive system state to be synchronized with a linear response combination of the response system states. The method, based on the Lyapunov stability theory and the pole placement technique, presents some useful features: (i) it enables synchronization to be achieved for both cases of $n < m$ and $n > m$; (ii) it is rigorous, being based on theorems; (iii) it can be readily applied to any chaotic (hyperchaotic) maps defined to date. Finally, the capability of the approach is illustrated by synchronization examples between the two-dimensional Hénon map (as the drive system) and the three-dimensional hyperchaotic Wang map (as the response system), and the three-dimensional Hénon-like map (as the drive system) and the two-dimensional Lorenz discrete-time system (as the response system).

Keywords: chaotic map, full state hybrid projective synchronization, inverse problem, maps with different dimensions

PACS: 05.45.–a, 05.45.Xt **DOI:** 10.1088/1674-1056/25/9/090503

1. Introduction

The topic of controlling a chaotic drive system and a driven (response) system to get synchronized dynamics has attracted great interest in nonlinear science.[1–31] Most of the methods that have been inspired by the Carroll and Pecora work[1] focus on complete (identical) synchronization, where two identical chaotic systems asymptotically approach the same trajectory.[2–6] Subsequently, different types of synchronization have been proposed in the literature.[8–10] Among them, the projective synchronization provides response system variables that are scaled replicas of the drive system variables.[7,8] Since the scaling factor is not predictable in Ref. [7], control methods have been successively developed for choosing any desired scaling factor.[8–13] A variation of projective synchronization is the so-called full state hybrid projective synchronization (FSHPS).[14–18] In this type of synchronization, the scaling factor can be different for each state variable, meaning that the single scaling parameter originally introduced in Ref. [7] is replaced by a diagonal scaling matrix. Recently, an interesting scheme[19] has been introduced, in which each response system state achieves synchronization with any arbitrary linear combination of drive system states. Since the adoption of an arbitrary scaling matrix represents a generalization of FSHPS (where the scaling matrix is a diagonal one), the method in Ref. [19] has been called arbitrary full-state hybrid projective synchronization (arbitrary FSHPS).

Based on these considerations, this paper presents a new synchronization scheme, with which each drive system state synchronizes with a linear combination of response system states. Since the drive system states and the response system states are inverted with respect to the arbitrary FSHPS, the proposed scheme is called inverse full-state hybrid projective synchronization (IFSHPS). The approach presents some useful features: (i) it enables chaotic (hyperchaotic) maps with different dimensions to be synchronized; (ii) it is rigorous, being based on theorems; (iii) it can be applied to a wide class of chaotic (hyperchaotic) maps.

The paper is organized as follows. In Section 2, the definition of inverse full state hybrid projective synchronization is introduced. In Section 3, two theorems are proved, which enable synchronization between n-dimensional and m-dimensional maps to be achieved for the $n < m$ and $n > m$ cases, respectively. Finally, the capability of the method is illustrated by examples of IFSHPS between the two-dimensional Hénon map (as the drive system) and the three-dimensional hyperchaotic Wang map (as the response system), and the three-dimensional Hénon-like map (as the drive system) and the two dimensional Lorenz discrete-time system (as the response system).

2. Inverse full state hybrid projective synchronization

It is assumed that the drive and response chaotic (hyperchaotic) systems considered herein can be written, respec-

†Corresponding author. E-mail: ouannas_adel@yahoo.fr
‡Corresponding author. E-mail: giuseppe.grassi@unisalento.it

© 2016 Chinese Physical Society and IOP Publishing Ltd

tively, in the form

$$x_i(k+1) = \sum_{j=1}^{n} a_{ij}x_j(k) + f_i(\boldsymbol{X}(k)), \quad i = 1,2,\ldots,n, \tag{1}$$

$$y_i(k+1) = g_i(\boldsymbol{Y}(k)) + u_i, \quad i = 1,2,\ldots,m, \tag{2}$$

where $\boldsymbol{X}(k) = (x_i(k))_{1\le i\le n}$ and $\boldsymbol{Y}(k) = (y_i(k))_{1\le i\le m}$ are the state vectors of the drive system and the response system, respectively, $(a_{ij}) \in \mathbb{R}^{n\times n}$, $f_i : \mathbb{R}^n \to \mathbb{R}$, $i = 1,2,\ldots,n$, and $g_i : \mathbb{R}^m \to \mathbb{R}$, $i = 1,2,\ldots,m$ are nonlinear functions whereas u_i, $i = 1,2,\ldots,m$, are controllers.

The definition of inverse full-state hybrid projective synchronization for the coupled chaotic systems given in Eqs. (1) and (2) is given as follows.

Definition 1 The n-dimensional drive system $\boldsymbol{X}(k)$ and the m-dimensional response system $\boldsymbol{Y}(k)$ are in inverse full-state hybrid projective synchronization when, for an initial condition, there exist controllers u_i, $i = 1,2,\ldots,m$ and real constants a_{ij}, $i = 1,2,\ldots,n$, $j = 1,2,\ldots,m$ such that the synchronization errors

$$e_i(k) = x_i(k) - \sum_{j=1}^{m} a_{ij}y_j(k), \quad i = 1,2,\ldots,n \tag{3}$$

satisfy $\lim_{k\to+\infty} e_i(k) = 0$ for $i = 1,2,\ldots,n$.

Remark 1 According to condition (3), it follows that in IFSHPS, each drive system state $x_i(k)$ synchronizes with a linear combination of response system states $a_{i1}y_1(k) + a_{i2}y_2(k) + \cdots + a_{im}y_m(k)$ for $i = 1,2,\ldots,n$. Recall that in arbitrary FSHPS each response system state achieved synchronization with a linear combination of drive system states. By comparing the definitions of the two schemes, it can be deduced that herein the roles of the drive system states and response system states have been inverted with respect to those in the arbitrary FSHPS.[19] This clarifies the reason why the proposed scheme has been called inverse full-state hybrid projective synchronization.

The error system (3) between the drive system (1) and the response system (2) can be derived as

$$\begin{aligned} e_i(k+1) = {} & \sum_{j=1}^{m} a_{ij}x_j(k) + f_i(\boldsymbol{X}(k)) \\ & - \sum_{j=1}^{m} a_{ij}(g_j(\boldsymbol{Y}(k)) + u_j). \end{aligned} \tag{4}$$

Two different cases will now be discussed, i.e., $n < m$ and $n > m$.

2.1. Case 1: $n < m$

In this case, the error system described by Eq. (4) can be written as

$$\begin{aligned} e_i(k+1) = {} & \sum_{j=1}^{n} (a_{ij} - l_{ij})e_j + R_i - \sum_{j=1}^{m} a_{ij}u_j, \\ & i = 1,2,\ldots,n, \end{aligned} \tag{5}$$

where $(l_{ij})_{1<i,j<n}$ are the control constants and

$$\begin{aligned} R_i = {} & \sum_{j=1}^{n} a_{ij}x_j(k) + f_i(\boldsymbol{X}(k)) + \sum_{j=1}^{m} (l_{ij} - a_{ij})e_j \\ & - \sum_{j=1}^{m} a_{ij}g_j(\boldsymbol{Y}(k)), i = 1,2,\ldots,n. \end{aligned}$$

Rewrite the error system in a compact form as

$$\boldsymbol{e}(k+1) = (\boldsymbol{A} - \boldsymbol{L})\boldsymbol{e}(k) + \boldsymbol{R} - \boldsymbol{\alpha}\boldsymbol{U}, \tag{6}$$

where $\boldsymbol{e}(k) = (e_i(k))_{1<i<n}$, $\boldsymbol{A} = (a_{ij})_{n\times n}$, $\boldsymbol{L} = (l_{ij})_{n\times n}$, $\boldsymbol{R} = (R_i)_{1\le i\le n}$, $\boldsymbol{\alpha} = (\alpha_{ij})_{n\times m}$, and $\boldsymbol{U} = (u_1,u_2,\ldots,u_m)^{\mathrm{T}}$.

In order to achieve IFSHPS between systems (1) and (2), the controller $\boldsymbol{U}$ is chosen as

$$\boldsymbol{U} = (u_1,u_2,\ldots,u_n,0,\ldots,0)^{\mathrm{T}}. \tag{7}$$

By substituting Eq. (7) into Eq. (6), the error system (6) can be written as

$$\boldsymbol{e}(k+1) = (\boldsymbol{A} - \boldsymbol{L})\boldsymbol{e}(k) + \boldsymbol{R} - \boldsymbol{\alpha}_1\boldsymbol{U}_1, \tag{8}$$

where $\boldsymbol{\alpha}_1 = (\alpha_{ij})_{n\times n}$ and $\boldsymbol{U}_1 = (u_i)_{1<i<n}$.

Theorem 1 For an invertible matrix $\boldsymbol{\alpha}_1$, IFSHPS between the drive system (1) and the response system (2) will occur if the following conditions are satisfies:

(i) $\boldsymbol{U}_1 = \boldsymbol{\alpha}_1^{-1}\boldsymbol{R}$, where $\boldsymbol{\alpha}_1^{-1}$ is the inverse matrix of $\boldsymbol{\alpha}_1$;

(ii) $(\boldsymbol{A} - \boldsymbol{L})^{\mathrm{T}}(\boldsymbol{A} - \boldsymbol{L}) - \boldsymbol{I}$ is a negative definite matrix.

Proof By substituting the control law (i) into Eq. (8), the error dynamics are described by

$$\boldsymbol{e}(k+1) = (\boldsymbol{A} - \boldsymbol{L})\boldsymbol{e}(k). \tag{9}$$

By selecting the candidate Lyapunov function in the form

$$\boldsymbol{V}(\boldsymbol{e}(k)) = \boldsymbol{e}^{\mathrm{T}}(k)\boldsymbol{e}(k), \tag{10}$$

it follows that

$$\begin{aligned} \Delta\boldsymbol{V}(\boldsymbol{e}(k)) = {} & \boldsymbol{e}^{\mathrm{T}}(k+1)\boldsymbol{e}(k+1) - \boldsymbol{e}^{\mathrm{T}}(k)\boldsymbol{e}(k) \\ = {} & \boldsymbol{e}^{\mathrm{T}}(k)(\boldsymbol{A} - \boldsymbol{L})^{\mathrm{T}}(\boldsymbol{A} - \boldsymbol{L})\boldsymbol{e}(k) - \boldsymbol{e}^{\mathrm{T}}(k)\boldsymbol{e}(k) \\ = {} & \boldsymbol{e}^{\mathrm{T}}(k)\left[(\boldsymbol{A} - \boldsymbol{L})^{\mathrm{T}}(\boldsymbol{A} - \boldsymbol{L}) - \boldsymbol{I}\right]\boldsymbol{e}(k). \end{aligned}$$

By using (ii), we obtain $\Delta\boldsymbol{V}(\boldsymbol{e}(k)) < 0$. Thus, from the Lyapunov stability theory, it can be readily shown that $\lim_{k\to+\infty} e_i(k) = 0$, $i = 1,2,\ldots,n$, indicating that the zero solution of the error system (9) is globally asymptotically stable. As a consequence, systems (1) and (2) are globally IFSHP synchronized.

2.2. Case 2: $m < n$

Now, the error system between the drive system (1) and the response system (2) can be described as

$$e_i(k+1) = \sum_{j=1}^{n}(a_{ij}-c_{ij})e_j + T_i - \hat{u}_i, \quad i = 1,2,\ldots,n, \tag{11}$$

where $(c_{ij})_{1\le i,j\le n}$ are the control constants,

$$T_i = \sum_{j=1}^{n} a_{ij}x_j(k) + f_i(\boldsymbol{X}(k)) + \sum_{j=1}^{m}(c_{ij}-a_{ij})e_j - \sum_{j=1}^{m}\alpha_{ij}g_j(\boldsymbol{Y}(k)), \quad i = 1,2,\ldots,n,$$

and $\hat{u}_i = \sum_{j=1}^{m}\alpha_{ij}u_j$ are new controllers $(i = 1,2,\ldots,n)$. Then, the error system (11) can be rewritten in a compact form as

$$\boldsymbol{e}(k+1) = (\boldsymbol{A}-\boldsymbol{C})\boldsymbol{e}(k) + \boldsymbol{T} - \boldsymbol{U}_2, \tag{12}$$

where

$$\boldsymbol{C} = (c_{ij})_{n\times n}, \quad \boldsymbol{T} = (T_i)_{1\le i\le n}, \quad \boldsymbol{U}_2 = (\hat{u_1},\hat{u_2},\ldots,\hat{u_n}),$$

and α_{ij} $(i = 1,2,\ldots,n;\ j = m+1, m+2,\ldots,n)$ are assumed not all equal to zero.

Theorem 2 IFSHPS between the drive system (1) and the response system (2) will occur if the following conditions are satisfied:

(i) $\boldsymbol{U}_2 = \boldsymbol{T}$;

(ii) all eigenvalues of $\boldsymbol{A}-\boldsymbol{C}$ are strictly inside the unit circle.

Proof By substituting the control law (i) into Eq. (6), the error system can be written as

$$\boldsymbol{e}(k+1) = (\boldsymbol{A}-\boldsymbol{C})\boldsymbol{e}(k). \tag{13}$$

By taking into account the stability theory of linear discrete-time systems, if condition (ii) is satisfied, it follows that all the solutions of the error system (13) go to zero as $k\to\infty$. As a consequence, systems (1) and (2) are globally IFSHP synchronized.

3. Examples

In this section, two examples are used to show the effectiveness of the proposed approach.

3.1. Example 1: $n < m$

Herein, the chaotic two-dimensional Hénon map is selected as the drive system and the hyperchaotic three-dimensional Wang system is chosen as the response system. The Hénon map[32] is described by

$$\begin{pmatrix} x_1(k+1) \\ x_2(k+1) \end{pmatrix} = \begin{pmatrix} x_2(k)+1-ax_1^2(k) \\ bx_1(k) \end{pmatrix}, \tag{14}$$

and has a chaotic attractor, plotted in Fig. 1, when $(a,b) = (1.4,0.2)$.

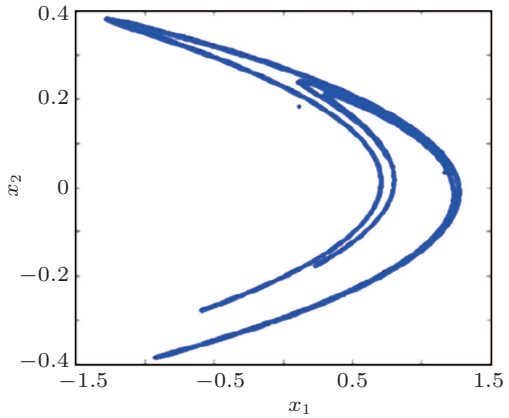


Fig. 1. (color online) Chaotic attractor of Hénon map in the (x_1,x_2) plane when $(a,b) = (1.4,0.2)$.

System (14) can be rewritten in the form $\boldsymbol{X}(k+1) = \boldsymbol{A}\boldsymbol{X}(k) + \boldsymbol{f}(\boldsymbol{X}(k))$ where

$$\boldsymbol{A} = \begin{pmatrix} 0 & 1 \\ b & 0 \end{pmatrix}, \quad \boldsymbol{f}(\boldsymbol{X}(k)) = \begin{pmatrix} 1-ax_1^2(k) \\ 0 \end{pmatrix}.$$

The hyperchaotic Wang system[33] can be described by

$$\begin{pmatrix} y_1(k+1) \\ y_2(k+1) \\ y_3(k+1) \end{pmatrix} = \begin{pmatrix} a_3y_2(k)+(a_4+1)y_1(k)+u_1 \\ a_1y_1(k)+y_2(k)+a_2y_3(k)+u_2 \\ (a_7+1)y_3(k)+a_6y_2(k)y_3(k)+a_5+u_3 \end{pmatrix}, \tag{15}$$

where u_1, u_2, and u_3 are the synchronization controllers. The uncoupled Wang system (15), obtained for $u_1 = u_2 = u_3 = 0$, has a hyperchaoticattractor[33] (plotted in Fig. 2) when $a_1 = 1.9$, $a_2 = 0.2$, $a_3 = 0.5$, $a_4 = 2.3$, $a_5 = 2$, $a_6 = 0.6$, and $a_7 = 1.9$.

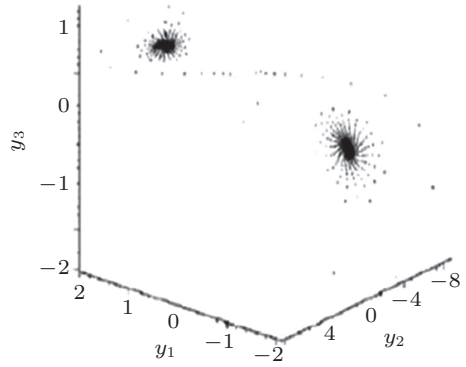


Fig. 2. Hyperchaotic attractor of the Wang system when $(a_1, a_2, a_3, a_4, a_5, a_6, a_7) = (1.9,0.2,0.5,2.3,2,0.6,1.9,1)$.

In this example, according to Eq. (15) and condition (i) of Theorem 1, the controllers $u_i, 1 \le i \le 3$, are obtained as follows:

$$\begin{cases} (u_1,u_2)^{\mathrm{T}} = \boldsymbol{\alpha}_1^{-1} \times [(-\boldsymbol{A}+\boldsymbol{L})\boldsymbol{e}(k) + \boldsymbol{A}\boldsymbol{X}(k) \\ \qquad\qquad -\boldsymbol{\alpha}\boldsymbol{g}(\boldsymbol{Y}(k))], \\ u_3 = 0, \end{cases} \tag{16}$$

where

$$\boldsymbol{\alpha} = \begin{pmatrix} 2 & 0 & 2 \\ 0 & 5 & 3 \end{pmatrix}, \quad \boldsymbol{\alpha}_1 = \begin{pmatrix} 2 & 0 \\ 0 & 5 \end{pmatrix},$$
$$\boldsymbol{\alpha}_1^{-1} = \begin{pmatrix} 0.5 & 0 \\ 0 & 0.2 \end{pmatrix}, \quad \boldsymbol{L} = \begin{pmatrix} 0.4 & 1 \\ b & -0.1 \end{pmatrix}.$$

The controllers (16) can be rewritten as

$$\begin{cases} u_1 = 0.2x_1(k) + 0.5x_2(k) - a_3y_2(k) \\ \qquad -(a_4+1.4)y_1(k) - (a_7+1.4)y_3(k) \\ \qquad -a_6y_2(k)y_3(k) - a_5, \\ u_2 = 0.2x_1(k) - 0.02x_2(k) - a_1y_1(k) \\ \qquad -0.9y_2(k) + (-0.6a_7 - 0.54 - a_2)y_3(k) \\ \qquad -0.6a_6y_2(k)y_3(k) - 0.6a_5, \\ u_3 = 0. \end{cases} \tag{17}$$

Note that, according to Theorem 1, it can be readily verified that $(\boldsymbol{A}-\boldsymbol{L})^{\mathrm{T}}(\boldsymbol{A}-\boldsymbol{L}) - \boldsymbol{I}$ is a negative definite matrix. Since Theorem 1 holds, it follows that the error system (9) is globally asymptotically stable and is described by $e_1(k+1) = -0.4e_1(k)$ and $e_2(k+1) = 0.1e_2(k)$. Thus, IFSHPS is achieved between the drive system (14) and the response system (15). Finally, note that in the proposed example of IFSHPS the errors $e_1(k)$ and $e_2(k)$ are

$$\begin{cases} e_1(k) = x_1(k) - (2y_1(k) + 2y_3(k)), \\ e_2(k) = x_2(k) - (5y_2(k) + 3y_3(k)). \end{cases} \tag{18}$$

Since $e_1(k)$ and $e_2(k)$ asymptotically approach zero (see Fig. 3), equation (18) highlights that each drive system state is synchronized with a linear combination of response systems states, indicating that IFSHPS has been successfully achieved.

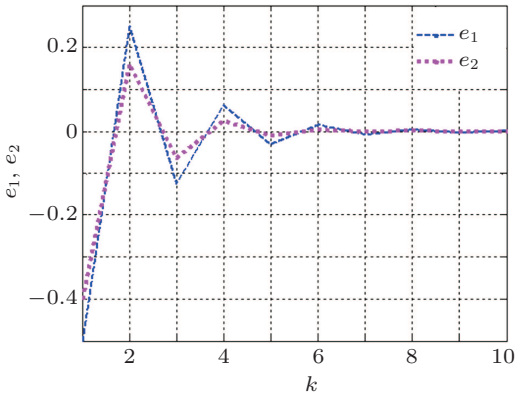


Fig. 3. (color online) Time evolution of the errors $e_1(k)$ and $e_2(k)$ between systems (14) and (15). According to Theorem 1, the errors asymptotically approach zero, indicating that IFSHPS is effectively achieved.

3.2. Example 2: $n > m$

Now, the hyperchaotic three-dimensional Hénon-like map is selected as the drive system and the chaotic two-dimensional Lorenz discrete-time system is chosen as the response system. The three-dimensional Hénon-like map[34] is described by

$$\begin{pmatrix} x_1(k+1) \\ x_2(k+1) \\ x_3(k+1) \end{pmatrix} = \begin{pmatrix} 1 + x_3(k) - ax_2^2(k) \\ 1 + bx_2(k) - ax_1^2(k) \\ bx_1(k) \end{pmatrix} \tag{19}$$

and has a hyperchaotic attractor (plotted in Fig. 4) when $(a,b) = (1.4, 0.2)$.

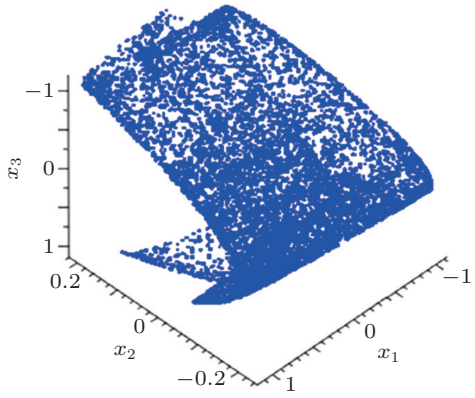


Fig. 4. (color online) Hyperchaotic attractor of the Hénon-like map (19) when $(a,b) = (1.4, 0.2)$.

System (19) can be rewritten in the form $\boldsymbol{X}(k+1) = \boldsymbol{A}\boldsymbol{X}(k) + \boldsymbol{f}(\boldsymbol{X}(k))$, where

$$\boldsymbol{A} = \begin{pmatrix} 0 & 0 & 1 \\ 0 & b & 0 \\ b & 0 & 0 \end{pmatrix}, \quad \boldsymbol{f}(\boldsymbol{X}(k)) = \begin{pmatrix} 1 - ax_2^2(k) \\ 1 - ax_1^2(k) \\ 0 \end{pmatrix}.$$

The controlled Lorenz discrete-time system[35] can be described as

$$\begin{pmatrix} y_1(k+1) \\ y_2(k+1) \end{pmatrix} = \begin{pmatrix} (1+a_1a_2)y_1(k) - a_2y_1(k)y_2(k) + u_1 \\ (1-a_2)y_2(k) + a_2y_2^2(k) + u_2 \end{pmatrix}, \tag{20}$$

where $\boldsymbol{U} = (u_1,u_2)^{\mathrm{T}}$ is the vector controller. The uncoupled Lorenz discrete-time system, obtained for $u_1 = u_2 = 0$, has a chaotic attractor[35,36] (plotted in Fig. 5) when $(a_1,a_2) = (1.25, 0.75)$.

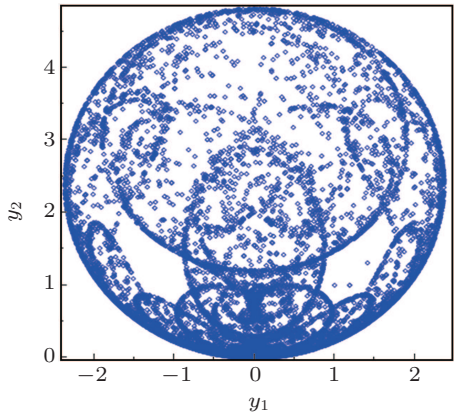


Fig. 5. (color online) Chaotic attractor of the Lorenz discrete-time system in the (y_1, y_2)) plane when $(a_1, a_2) = (1.25, 0.75)$.

In this example, the scaling constant matrix $\boldsymbol{\alpha} = (\alpha_{ij})_{3\times 2}$ and the control matrix $\boldsymbol{C} = (c_{ij})_{3\times 3}$ are chosen as

$$\boldsymbol{\alpha} = \begin{pmatrix} 2 & 1 \\ 3 & 2 \\ 1 & 3 \end{pmatrix}, \quad \boldsymbol{C} = \begin{pmatrix} 0.1 & 0 & 1 \\ 0 & 0 & 0 \\ b & 0 & 0.3 \end{pmatrix}.$$

Then, according to condition (i) of Theorem 2, the control law is given by

$$\begin{cases} 2u_1 + u_2 = T_1, \\ 3u_1 + 2u_2 = T_2, \\ u_1 + 3u_2 = T_3, \end{cases} \tag{21}$$

where

$$\begin{cases} T_1 = 0.1e_1(k) + x_3(k) + 1 - ax_2^2(k) \\ \quad -2(1 + a_1a_2)y_1(k) + 2a_2y_1(k)y_2(k) \\ \quad -(1 - a_2)y_2(k) - a_2y_2^2(k), \\ T_2 = -be_2(k) + 1 + bx_2(k) - ax_1^2(k) \\ \quad -3(1 + a_1a_2)y_1(k) + 3a_2y_1(k)y_2(k) \\ \quad -2(1 - a_2)y_2(k) - 2a_2y_2^2(k), \\ T_3 = 0.3e_2(k) + bx_1(k) \\ \quad -(1 + a_1a_2)y_1(k) + a_2y_1(k)y_2(k) \\ \quad -3(1 - a_2)y_2(k) - 3a_2y_2^2(k). \end{cases}$$

So, the control input can be rewritten as

$$\begin{cases} u_1 = \frac{1}{4}(T_1 + T_2 - T_3), \\ u_2 = \frac{1}{2}(T_1 - T_2 + T_3). \end{cases} \tag{22}$$

According to Theorem 2, it can be readily verified that all the eigenvalues of $(\boldsymbol{A} - \boldsymbol{C})$ are strictly inside the unit circle. Since Theorem 2 holds, it follows that the error system (13) is globally asymptotically stable and is described by $e_1(k+1) = -0.1e_1(k)$, $e_2(k+1) = 0.2e_2(k)$, and $e_3(k+1) = -0.3e_3(k)$. Thus, IFSHPS is achieved between the drive system (19) and the response system (20). Finally, note that in the proposed example of IFSHPS, the errors $e_1(k)$, $e_2(k)$, and $e_3(k)$ are

$$\begin{cases} e_1(k) = x_1(k) - (2y_1(k) + y_2(k)), \\ e_2(k) = x_2(k) - (3y_1(k) + 2y_2(k)), \\ e_3(k) = x_3(k) - (y_1(k) + 3y_2(k)). \end{cases} \tag{23}$$

Since $e_1(k)$, $e_2(k)$, and $e_3(k)$ asymptotically approach zero (see Fig. 6), equation (23) highlights that each drive system state is synchronized with a linear combination of response systems states, indicating that IFSHPS has been successfully achieved.

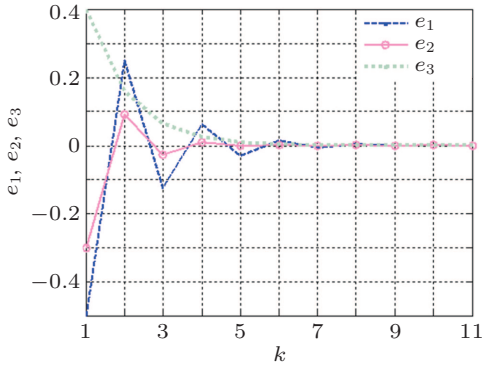


Fig. 6. (color online) Time evolution of the errors $e_1(k)$, $e_2(k)$, and $e_3(k)$ between systems (19) and (20). According to Theorem 2, the errors asymptotically approach zero, indicating that IFSHPS is effectively achieved.

4. Discussion

Referring to chaotic discrete-time systems, herein comparisons are carried out between the proposed approach and a number of synchronization methods in the literature, with the aim to show the advantages and the novelty of the conceived scheme.

In Ref. [27], attention was mainly focused on the full-state hybrid projective synchronization and related issues, with application to 2D discrete-time systems. Even though the theoretical approach developed in Ref. [27] is interesting, being based on nonlinear control method and Lyapunov stability, the proofs of the synchronization schemes are limited to 2D discrete-time systems only. This is further confirmed by simulation results, which focus on 2D systems only, i.e., the Fold discrete-time system (drive system) and the Lorenz discrete-time system (response system), which are both two-dimensional systems.[27] On the other hand, the technique proposed herein enables inverse full-state hybrid projective synchronization to be achieved for n-dimensional drive systems and m-dimensional response systems. As a consequence, the approach developed herein is much more general than the one illustrated in Ref. [27].

In Ref. [28], the issue of generalized synchronization (GS), along with its inverse problem, was discussed with reference to discrete-time systems. In GS, two chaotic systems are said to be synchronized if there exists a functional relationship Φ between the drive system states and the response system states.[28] However, the synchronization schemes discussed in Ref. [28] are very different from those proposed herein. Namely, in this paper, we do not consider any functional relationship Φ between drive and response systems. According

to the IFSHPS schemes developed herein, each n-dimensional drive system state synchronizes with a linear combination of m-dimensional response system states. This holds for both cases of $n < m$ and $m > n$.

Finally, in Ref. [29], the problem of inverse matrix projective synchronization (IMPS) for different dimensional chaotic systems in discrete-time was investigated. In this type of synchronization, the drive system and the response system synchronize up to a special scaling matrix, as shown through the examples reported in Ref. [29]. It can be argued that, while the synchronization criteria reported in Ref. [29] are restricted to specific scaling matrices, in this paper a general IFSHPS approach is developed, where each drive system state synchronizes with any arbitrary linear combination of response system states. In conclusion, the approach developed herein is much more general than the one illustrated in Ref. [29], since arbitrary scaling matrices can be exploited to achieve IFSHPS.

5. Conclusion

We have illustrated a new scheme to achieve chaos (hyperchaos) synchronization in discrete-time between a drive system of dimension n and a response system of dimension m. The proposed approach, which enables each drive system state to be synchronized with a linear response combination of response system states, has shown some remarkable features. Namely, by exploiting the Lyapunov stability theory and the pole placement technique, synchronization is rigorously proved to be achievable for any chaotic (hyperchaotic) map defined to date, including the two cases $n < m$ and $n > m$. Finally, the effectiveness of the method has been illustrated by synchronizing a two-dimensional chaotic Hénon map with a three-dimensional hyperchaotic Wang map, and a three-dimensional hyperchaotic Hénon-like map with a two-dimensional chaotic discrete-time Lorenz system.

References

[1] Carroll T L and Pecora L M 1991 *IEEE Trans. Circuits Syst.* **38** 453
[2] Brucoli M, Carnimeo L and Grassi G 1996 *Int. J. Bifurcat. Chaos* **6** 1673
[3] Grassi G and Mascolo S 1997 *IEEE Trans. Circuits Syst. I* **44** 1011
[4] Grassi G and Mascolo S 1998 *IEE Electron Lett.* **34** 424
[5] Brucoli M, Cafagna D, Carnimeo L and Grassi G 1998 *Int. J. Bifurcat. Chaos* **8** 2031
[6] Grassi G and Mascolo S. 1999 *IEEE Trans. Circuits Syst. II* **46** 478
[7] Manieri R and Rehacek J 1999 *Phys. Rev. Lett.* **82** 3042
[8] Chee C Y and Xu D 2003 *Phys. Lett. A* **318** 112
[9] Xu D 2001 *Phys. Rev. E* **63** 2
[10] Xu D and Chee C Y 2002 *Phys. Rev. E* **66** 046218
[11] Grassi G and Miller D A 2009 *Chaos Soliton. Fract.* **39** 1246
[12] Grassi G and Miller D A 2007 *Int. J. Bifur. Chaos* **17** 1337
[13] Niu Y J, Wang X Y, Nian F Z and Wang M J 2010 *Chin. Phys. B* **19** 120507
[14] Hu M, Xu Z, Zhang R and Hu A 2007 *Phys. Lett. A* **365** 315
[15] Zhang Q and Lu J 2008 *Phys. Lett. A* **372** 1416
[16] Hu M, Xu Z, Zhang R and Hu A 2007 *Phys. Lett. A* **361** 231
[17] Hu M, Xu Z and Zhang R 2008 *Comm. Nonlinear Science Num. Simulations* **13** 456
[18] Hu M, Xu Z and Zhang R 2008 *Comm. Nonlinear Science Num. Simulations* **13** 782
[19] Grassi G 2012 *Chin. Phys. B* **21** 060504
[20] Han F, Wang Z J, Fan H and Gong T 2015 *Chin. Phys. Lett.* **32** 40502
[21] Wang S T, Wu Z M, Wu J G, Zhou L and Xia G Q 2015 *Acta Phys. Sin.* **64** 154205 (in Chinese)
[22] Ren H P and Bai C 2015 *Chin. Phys. B* **24** 80503
[23] Wei W and Zuo M 2015 *Chin. Phys. B* **24** 80501
[24] Liu S, Wang Z L, Zhao S S, Li H B and Xiong L J 2015 *Chin. Phys. B* **24** 74501
[25] Shu J 2015 *Chin. Phys. B* **24** 60509
[26] Yang F, Wang G Y and Wang X Y 2015 *Chin. Phys. B* **24** 60506
[27] Ouannas A 2014 *J. Nonlinear Dynamics* 983293
[28] Ouannas A and Odibat Z 2015 *Nonlinear Dynamics* **81** 765
[29] Ouannas A and Mahmoud E E 2014 *Journal Computational Intelligence and Electronic Systems* **3** 188
[30] Danca M F and Tang W K S 2016 *Chin. Phys. B* **25** 010505
[31] Wang Y, Cai B Z, Jin P P and Hu T L 2016 *Chin. Phys. B* **25** 010503
[32] Hénon M 1976 *Comm. Math. Phys.* **50** 69
[33] Wang X Y 2003 *Chaos in Complex Nonlinear Systems* (Beijing: Publishing House of Electronics Industry)
[34] Stefanski K 1998 *Chaos Soliton. Fract.* **9** 83
[35] Itoh M, Yang T and Chua L O 2001 *Int. J. Bifurcation Chaos* **11** 551
[36] Grassi G 2012 *Chin. Phys. B* **21** 050505